ACS Catalysis

Review

pubs.acs.org/acscatalysis

Catalysis Chemistry of Dimethyl Ether Synthesis

Jian Sun, Guohui Yang, Yoshiharu Yoneyama, and Noritatsu Tsubaki*

Department of Applied Chemistry, School of Engineering, University of Toyama, Gofuku 3190, Toyama 930-8555, Japan

ABSTRACT: Dimethyl ether (DME) is receiving great attention as a clean alternative fuel, owing to the increasing energy demand. Despite tremendous efforts, catalytic synthesis of DME via a high efficient route remains a great challenge. Catalyst design is at the heart of enhancing the catalytic efficiency of DME synthesis. In this paper, we pay close attention to recent advances on the evolution of catalysts for direct dehydration from methanol and for the tandem catalysis from synthesis gas (syngas). The progress in metal deposition mode, support modification, and reaction routes is encouraging in recent years. In addition, significant challenges and future research scope in DME synthesis are focused as well.

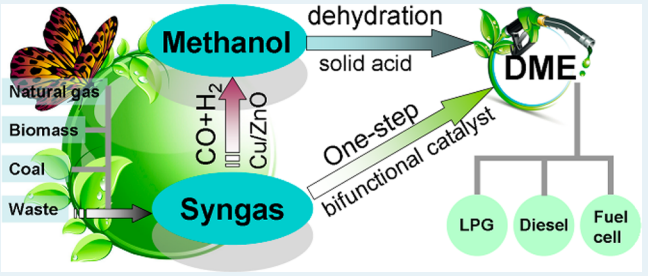

KEYWORDS: *dimethyl ether, methanol, syngas, zeolite, catalyst, bifunctional*

1. INTRODUCTION

Dimethyl ether (DME) is the simplest ether, without a C−C bond. It is one of the hot research areas in energy chemistry and environmental chemistry recently.[1] DME can take the place of LPG due to its similar physicochemical property. Besides, DME can also be used as diesel fuel of high cetane number, especially with very low soot emission in the exhaust gas from a diesel engine as it has no C−C bond structure. It can be readily decomposed even if being leaked into air and is very safe and benign to the environment.

DME is not only used as a final product but also employed to be converted to many chemicals and energy products. With very low poison property, DME often plays an alternative role to methanol. DME can be converted into light olefins and aromatics with a zeolite catalyst.[2] It also serves as a hydrogen source for fuel cells. Acting as a hydrogen carrier, it can be reformed again to syngas ($CO+H_2$) or hydrogen if necessary. In some cases, DME can be oligomerized to dimethoxymathane ($CH_3OCH_2OCH_3$, DMM) or polyoxymethylene dimethyl ethers (DMMn),[3] which are liquid diesel fuels under room temperature and atmospheric pressure. Furthermore, DME is a key product or intermediate in C1 chemistry or methane/syngas chemistry. It can be catalytically transformed to methyl acetate,[4] formaldehyde,[5] and ethanol,[6] via reaction with CO or syngas (a mixture of CO and H_2).

Currently, catalytic synthesis of DME can be simply realized from methanol dehydration over an acid support or from syngas conversion via a two-step reaction with methanol as an intermediate, as shown in Figure 1. Since syngas is produced from natural gas, coal, coal-bed methane, biomass, and other waste resources, DME is in the spotlight as a biofuel from the viewpoint of sustainability.[7] As a commercial methanol production method from syngas, using the ICI process being operated under high temperature such as 573 K, it has very low one-pass reactant conversion due to severe thermodynamic limitation on this exothermal reaction.[8,9] Direct DME synthesis

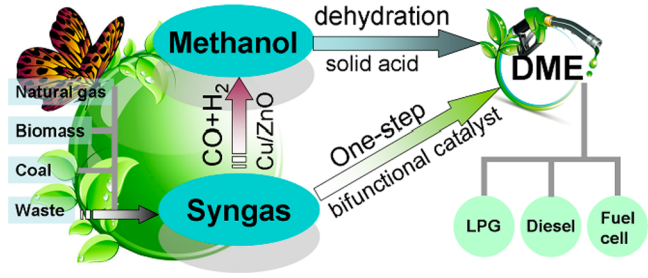

Figure 1. Route of DME synthesis from methanol or syngas.

from CO_2-containing syngas is of great importance, where methanol synthesis from CO_2-containing syngas is coupled *in situ* with methanol dehydration to the DME reaction. This scavenger effect on methanol can lower the catalyst surface concentration of the intermediate methanol and break the thermodynamic limitation on the overall CO conversion. Consequently CO conversion in the direct DME synthesis can be up to 80% in fixed bed reactor or slurry-phase process, significantly higher than that in a regular methanol synthesis such as 20%.

In view of the rapid progress and increasing achievements of DME synthesis in recent years, a detailed and critical review is greatly indispensable to completely cover the flourishing field and motivate further scientific activities. To the best of our knowledge, only a few perspective papers were published regarding the catalytic synthesis of DME.[7,10−12] In this review, we focus on the development of two different routes for DME synthesis, including direct methanol dehydration and syngas one-step conversion. Evolution of methanol dehydration on Al_2O_3 or a zeolite catalyst is demonstrated in the first part. More

Received: July 7, 2014
Revised: August 21, 2014
Published: August 21, 2014

   dx.doi.org/10.1021/cs500967j | ACS Catal. 2014, 4, 3346−3356

importantly, the progress on one-step conversion from syngas to DME is emphasized due to the increasing attention worldwide. Beyond that, significant challenges and future research scope in DME synthesis are mentioned as well.

2. DME SYNTHESIS FROM METHANOL

2.1. DME Synthesis from Methanol on a γ-Al_2O_3 Catalyst. DME synthesis can be achieved directly from methanol vapor-phase dehydration (methanol to DME, MTD) over different solid-acid catalysts, such as conventional γ-Al_2O_3,[13−15] acidic zeolite[16,17] (HZSM-5, HY, HZSM-22, and H-SAPO), heteropolyacid,[18] and composite oxides[19,20] (SiO_2−Al_2O_3 and ZrO_2−TiO_2) or from liquid-phase dehydration with sulfuric acid.[7] Generally, γ-Al_2O_3 is recognized as the most efficient one owing to its low cost, high DME selectivity, excellent lifetime, and high mechanical resistance among the above catalysts. In addition to the MTD process, the catalytic dehydration process on γ-Al_2O_3 is also widely used in production of alkenes and ethers from various alcohols due to its suitable acidity.[21−23]

Recently, Yoo et al. investigated the influence of physical properties of alumina on the catalytic performance of MTD.[24] Different alumina materials were compared after heat treatment. The result demonstrated that besides the acidity, the structure type of alumina catalyst is a key factor to MTD reactions as well. The η-Al_2O_3 with the preferentially exposed (111) surface is superior to γ-Al_2O_3 with (110) surface. In the latest report,[14] Kondarides et al. also mentioned a similar viewpoint. The authors indicated that catalytic behavior of the MTD process is strongly dependent on the textural properties, degree of crystallinity, and total amount of acid sites of Al_2O_3. The ammonia uptake on per gram of catalyst depends strongly on specific surface area (SSA) of the sample and increases linearly with an increase of SSA, as indicated in Figure 2. More

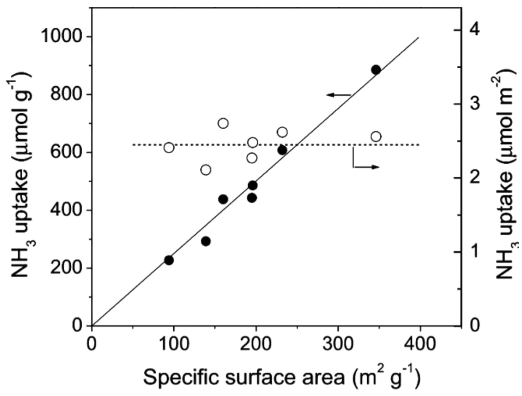

Figure 2. Amount of ammonia desorbed in NH_3-TPD experiments as a function of the specific surface area of Al_2O_3 catalysts. Reproduced with permission from ref 14. Copyright 2014 Elsevier.

interestingly, the density of surface acid sites is approximately the same for all the alumina samples, if the data are expressed per unit surface area. The MTD performance will be greatly promoted if the specific surface area of catalyst is increased, but the alumina with excessively higher porosity or smaller crystallite size is less active in such a reaction.

Undoubtedly, alumina is an excellent candidate for the methanol dehydration process as proven by many reports. However, its unsolved drawbacks are also obvious, such as low hydrothermal activity, many side reactions, competitive adsorption of steam resulting from the strong surface hydrophilic ability, etc. Lately, numerous researchers have performed a series of effective works to develop an active, selective, and stable alumina-based MTD catalyst. Modification with another oxide is considered as one of the most powerful approaches to improve the MTD performance on conventional γ-Al_2O_3.

Yaripour et al. compared the performance of pure Al_2O_3 and a silica-modified Al_2O_3 catalyst.[15] The researchers found that the latter showed higher methanol conversion than the former by means of the promotion of surface acidity and surface area. Compared with the unmodified alumina catalyst on which methane is the main byproduct, the optimized SiO_2-modified catalyst exhibited better activity and no byproduct in the final product. In parallel, a phosphorus-modified γ-Al_2O_3 catalyst was also reported by the group, exhibiting similar promoted influence in MTD reactions as compared to an unmodified one.[25,26] Liu et al. developed an effective Nb_2O_5-modified alumina catalyst.[13] They reported that the conversion of methanol was clearly enhanced after Nb_2O_5 modification. The strength of acid sites was reduced, but the number of acid sites was obviously increased by the modification. The optimized amount of Nb_2O_5 in alumina catalyst was about 10 wt %. The addition of other crystallite of alumina into γ-Al_2O_3 was observed to play a similar role in promoting the MTD performance.

Beyond that, mixing with another crystallite alumina with γ-Al_2O_3 can produce a promotion effect on MTD performance likewise. Khom-in et al. found that after a γ-Al_2O_3 catalyst was mixed with 20 wt % of χ-phase, the density and the strength of surface acidity of alumina were increased significantly, achieving a higher DME yield of 86% and stability than the unmixed pure γ-Al_2O_3 and χ-Al_2O_3 catalysts.[27]

2.2. DME Synthesis from Methanol on an Acidic Zeolite Catalyst. In addition to the conventional alumina, a series of zeolites, which are effective in most acidic catalysis, are commonly employed as dehydration catalysts for DME synthesis owing to their high hydrothermal stability and low-temperature availability.[17,28,29] In general, DME synthesis preferably proceeded on the weak and moderate acidic sites of a solid-acid catalyst.[15,19,30] However, considerable byproducts in DME synthesis such as hydrocarbons and even coke can be produced on these catalysts with the existence of strong acid sites on those acidic zeolites, thus lowering the productivity of methanol dehydration to DME. Accordingly, it is very necessary to adjust and modify the acidity of zeolite by embedding other elements in order to enhance the DME selectivity and catalytic stability.

It is important to point out that the dilution of strong acid sites can be achieved by Na^+ ions modification in zeolite framwork.[31,32] Recently, sodium-modified HZSM-5 zeolite of a high MTD catalytic performance is reported by Jun et al., in terms of activity, selectivity, and stability over a wide range of temperatures (230−340 °C).[31] The strong surface acid sites were partially substituted by Na ions in HZSM-5, realizing the prevention of byproduct formation of coke and hydrocarbons. Additionally, rare earth metals are important modifiers for zeolite as behaved in many other catalysis fields according to recent related works.[33−35] Hou et al. prepared various rare earth metals (La, Ce, Pr, Nd, Sm, and Eu) decorated Y zeolite via the ion-exchange method.[36] The result demonstrated that rare earth metals were encapsulated in the supercage of zeolite Y. The La and Ce modified zeolites exhibited a high proportion of moderate-strength acid sites and were more active and stable for methanol dehydration to DME.

dx.doi.org/10.1021/cs500967j | ACS Catal. 2014, 4, 3346−3356

It is also mentioned that the physical structure, mesoporosity, and crystal size of zeolite affect the MTD performance. The group of Xiao and Fei reported a useful aluminum fluoride modified HZSM-5 catalyst prepared by a mechanical mixture route.[17] All of the structure, texture, and acidity of a HZSM-5 zeolite could be efficiently adjusted by adding different amounts of AlF_3. A suitable adding amount (about 2 wt %) could increase both the content of framework aluminum and the surface area of HZSM-5, resulting in much higher activity and better stability than raw HZSM-5 in MTD reactions (shown in Figure 3). This

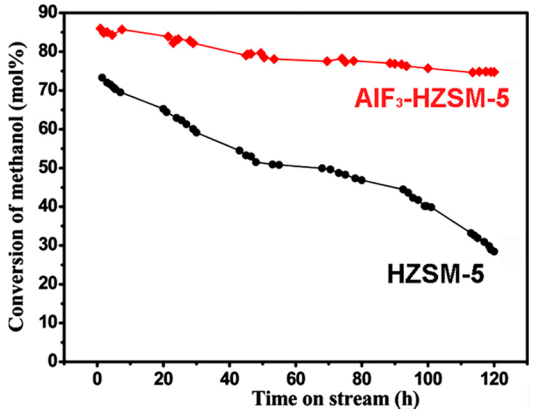

Figure 3. Conversion of methanol on stream on AlF_3-modified HZSM-5 and unmodified HZSM-5. Figure reproduced with permission from ref 17. Copyright 2012 American Chemical Society.

mild and facile route is important for industrial application by means of the solvent-free and effective use of fluoride reagents if compared with conventional fluoride modification route.[37−39] Rownaghi and co-workers investigated the effects of ZSM-5 crystal size and mesoporosity on the MTD performance.[40] In detail, the reaction activity is correlated with the zeolite crystal size, whereas the DME selectivity is dependent on acid site distribution on external surface and in the bulk of zeolite. Furthermore, the DME selectivity and catalyst stability were both promoted with the reduction of the crystal size, because of faster mass transfer of products from the zeolite crystals and pores. The authors indicated that ZSM-5 nanocrystals of uniform size were the most active and selective catalyst for methanol dehydration and DME production.

To further improve the thermostability of acidic zeolite in MTD reactions, zeolite can also be loaded on other porous and heat-stable support, as demonstrated by the recent work of Pham-Huu et al.[41] HZSM-5 zeolite was successfully supported on silicon carbide foam to fabricate a HZSM-5/SiC catalyst for the MTD reaction. The ^{29}Si magic-angle spinning (MAS) NMR spectrum confirmed formation of the zeolite on the SiC surface (Figure 4a). The supported zeolite microparticles were uniform in size and highly dispersed on the porous SiC support (Figure 4b), showing a highly selective and stable MTD performance. The mechanical anchorage of the zeolite layer on support was greatly enhanced due to the strong interface between the zeolite layer and silicon carbide, thus preventing the loss of zeolite during transport and reactions; and the excellent mass and heat transfer ability of SiC[41,42] resulted in greater accessibility of the reactants to the active sites as well as a higher resistance to deactivation by coke formation or by the presence of water. The design of supported acidic zeolite provided a novel strategy on optimizing the methanol dehydration process.

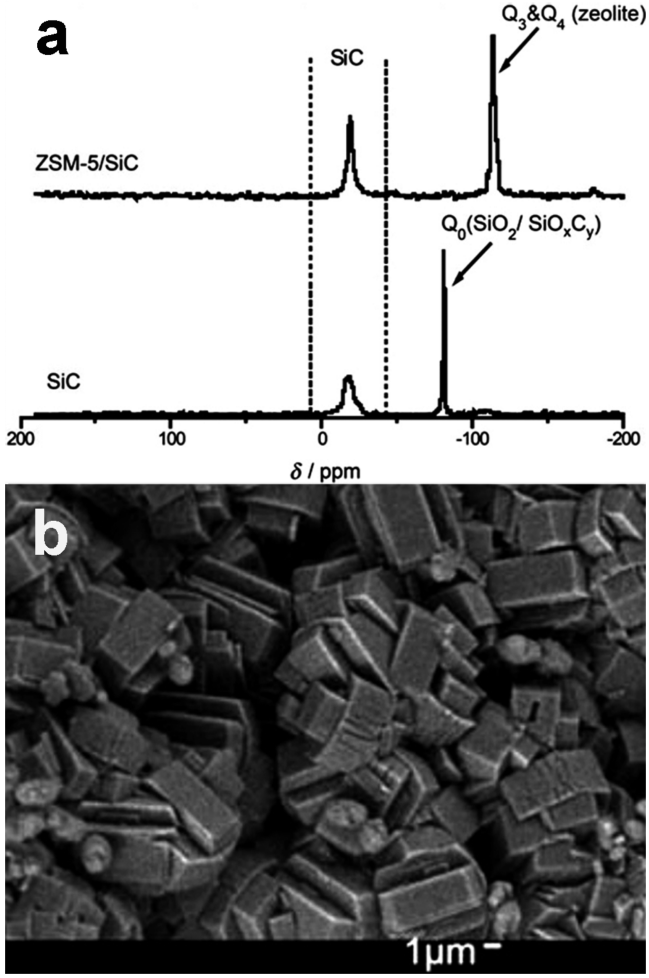

Figure 4. SiC supported HZSM-5 catalyst for DME synthesis. a) ^{29}Si MAS NMR spectrum of the SiC support after air calcination at 900 °C for 5 h and the supported zeolite; b) SEM images of the zeolite supported on SiC. Figures reproduced with permission from ref 41. Copyright 2008 WILEY-VCH Verlag GmbH & Co. KGaA, Weinheim.

2.3. Possible Kinetics and Mechanism of the MTD Process. Apart from the evolution of solid-acid catalysts, fractional recent advances focused on the possible kinetics and mechanism research of the MTD process.[16,43−46] A great deal of effort is still needed to investigate the reaction pathways due to the existence of some dispute currently. Based on relevant works, Ha et al. presented a new MTD reaction pathway,[43] in which two nondissociatively adsorbed methanol molecules with the acidic sites on zeolite are simultaneously involved in the first step of the mechanism to generate the intermediate molecule, which rearranges itself to split into the methyl carboxonium ion and carbenium ion at the same time or split into two methyl carboxonium ions. This key process is considered as the rate-determining step in the whole reactions.

Two different pathways from methanol to DME have been proposed, involving the associative and dissociative pathways.[47] It is well accepted that both of the two above proceed on Brønsted acid sites.[46,48] Recently, Nørskov and Mose demonstrated the MTD conversion over ZSM-22 Brønsted acid sites on the basis of periodic density functional theory (DFT) calculations.[16] The authors indicated that DME can be produced from methanol following either the faster dissociative or the slower associative pathway (Figure 5a), both of which showed

dx.doi.org/10.1021/cs500967j | ACS Catal. 2014, 4, 3346−3356

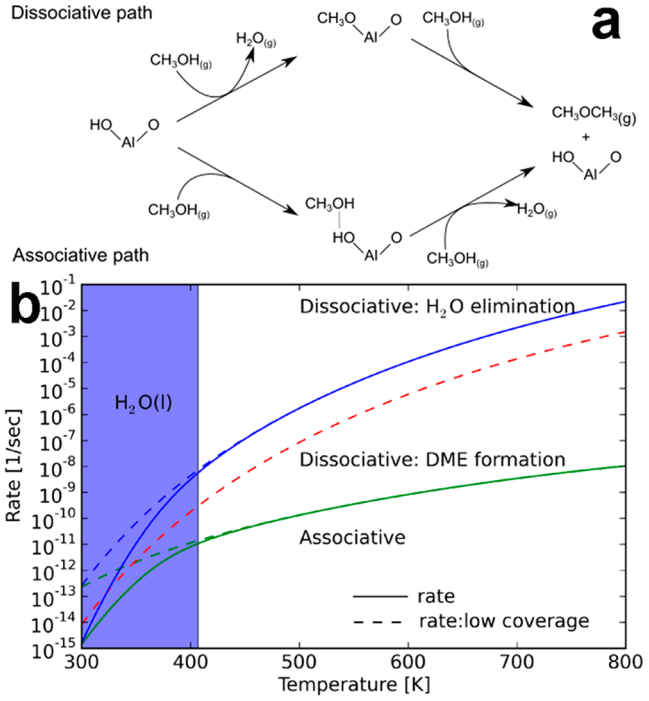

Figure 5. (a) The dissociative and the associative pathways for the MTD reaction. (b) The rate of the three different reactions in DME synthesis, calculated within the irreversible step approximation. The irreversible step approximation rate is calculated with or without assuming low coverage of methanol. Figures reproduced with permission from ref 16. Copyright 2013 American Chemical Society.

similar dependence on acidity. Moreover, water has no positive effect on the DME formation rate. The established linear correlations between acidity and activation energies suggested that weaker acids produced higher activation energies. In addition, the dissociative pathway involves two steps and the actual rate of DME formation is given by the slower one of the two steps. The rate of the DME formation step is always slower than that of the water elimination step (Figure 5b). Therefore, the rate of the dissociative pathway is determined by the DME formation step.

3. ONE-STEP DME SYNTHESIS FROM SYNGAS (CO, CO_2, AND H_2)

The MTD process is regarded as the most mature route and is widely used in chemical industries among DME synthesis routes. However, methanol is an expensive chemical feedstock, making DME cost much more to manufacture via the process.[49,50] By contrast, the syngas-to-DME (STD) process is promising and receiving increasing attention from researchers and industries worldwide in recent times. Syngas can be derived from biomass gasification,[51] natural gas partial oxidation or reforming,[52] coal gasification,[53] waste conversion,[54] etc.; therefore, the STD route is of dramatically economic value and sustainable significance. Generally, the indirect STD process involves the following two consecutive reactions, named as methanol synthesis and methanol dehydration, in parallel with the water gas shift process as a side reaction.

$$CO + 2H_2 \rightarrow CH_3OH \text{ (a)};$$

$$2CH_3OH \rightarrow CH_3OCH_3 + H_2O \text{ (b)};$$

$$CO + H_2O \rightarrow CO_2 + H_2 \text{ (c)}$$

On the other hand, in the case of CO_2-rich syngas as a starting feedstock instead of CO-rich syngas, the primary methanol synthesis reaction proceeded in terms of the CO_2 hydrogenation process: $CO_2 + 3H_2 \rightarrow CH_3OH + H_2O$ (d).[55,56]

Totally, the STD reaction is kinetically controlled by the Cu-catalyzed methanol synthesis reaction due to a higher rate of methanol dehydration between two primary reactions (a) and (b).[57] The tandem reactions from syngas to DME can be realized by a two-step reaction with a single Cu-based catalyst and a single solid-acid catalyst or by a one-step reaction with a single bifunctional catalyst in a fixed-bed, slurry-bed, or fluidized-bed reactor.[58] In one-step DME synthesis, the thermodynamic equilibrium constraint of syngas conversion in the two-step reactions was well broken,[59] currently drawing much attention worldwide. In this review, advances of the one-step DME synthesis are emphasized to review since it is becoming a hot topic of interest.

3.1. Hybrid Catalyst for the STD Process. The hybrid catalyst combining two separate types of active sites for the STD process is usually prepared by a simply physical mixing method and universally applied in STD reactions.[30,49,57,60−62] For the methanol synthesis, the Cu/ZnO-based catalyst has been developed successfully for several decades, and the reaction mechanism and effect of active ingredients are also well investigated.[8,63−66] For the methanol dehydration, the γ-Al_2O_3 and acidic zeolite are common components as mentioned in the previous section. The consecutive reactions on hybrid catalysts are more thermodynamically favorable, since methanol synthesis is generally severely limited by thermodynamics and immediate conversion of the produced methanol will maximize the syngas conversion.[49,67,68]

The crucial issue for preparing a high-active hybrid catalyst is optimizing the composition and reaction conditions of two functional components. It is also important to balance the acidity of zeolite by embedding other suitable basic oxides. Mao et al. prepared a hybrid catalyst for the STD reaction by physically mixing the CuO−ZnO−Al_2O_3 component and magnesium oxide modified HZSM-5 zeolite.[49] With the suitable amount of MgO addition, the selectivities of undesired byproducts such as hydrocarbons and CO_2 obtained from the further dehydration of DME were clearly decreased. As the unselective strong Brønsted acid sites were removed and Lewis acid sites were increased by modification, the DME yield was improved from 49% to higher than 64%. The process for methanol dehydration was possibly realized on both acidic and basic sites on magnesium oxide modified HZSM-5.

Besides, the modification with a metal oxide plays other role in STD reaction. Ji et al. mechanically mixed HZSM-5 zeolite with ZrO_2-modified CuO−Fe_2O_3 composite oxides at a 1:1 mass ratio to prepare an active catalyst for DME synthesis from CO_2 and H_2.[55] Zr doping could change the catalyst pore size, providing the best specific surface area when the ZrO_2 amount was 1.0 wt %, based on nitrogen adsorption−desorption isotherms (Figure 6a). Zr incorporation to the methanol synthesis catalyst can change the outer-shell electrons of Cu, enhance the reducing behavior of CuO, and increase the surface area and the number of active sites, thus clearly promoting the conversion of CO_2 and the yield of DME. During a 16 h reaction process, the CO_2

dx.doi.org/10.1021/cs500967j | ACS Catal. 2014, 4, 3346−3356

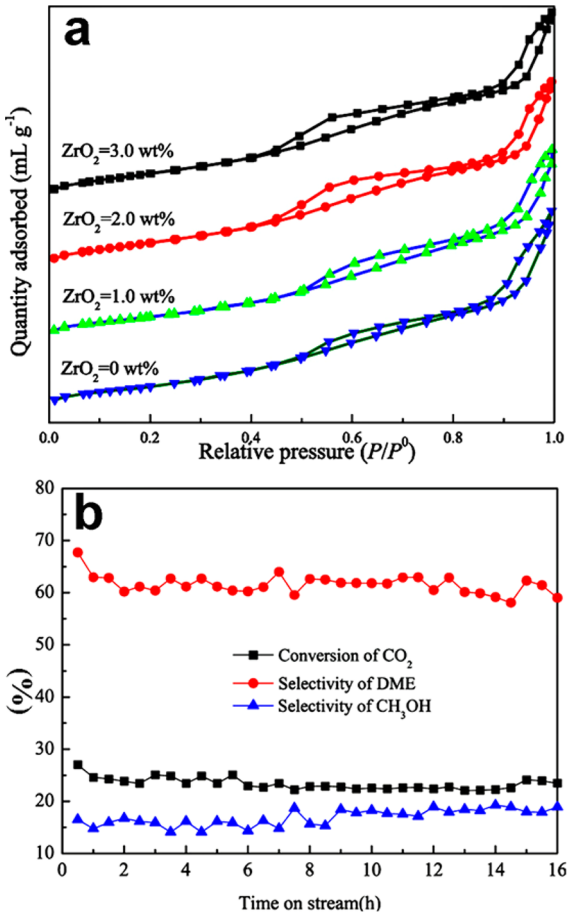

Figure 6. a) Nitrogen adsorption/desorption isotherms of CuO–Fe_2O_3–ZrO_2 composites with different ZrO_2 contents. b) Effects of the conversion of CO_2 and the selectivity of DME/CH_3OH with CuO–Fe_2O_3–ZrO_2/ HZSM-5 with time on stream. Reproduced with permission from ref 55. Copyright 2013 American Chemical Society.

conversion and DME/methanol selectivity remained nearly constant, as indicated in Figure 6b.

The interaction between two different active sites is another factor to impact the STD performance. García-Trenco et al. reported that the gradual deterioration of the methanol synthesis activity of the Cu/ZnO-based catalyst in the hybrid catalysts prepared by grinding was caused by detrimental interactions between Al species of zeolite and Cu sites of Cu/ZnO particles at the surface-contact of both components.[57] Up to now, the hybrid catalyst for STD reactions still shows some drawbacks, such as the far distance between two active sites, the low performance and the short reaction lifetime. Therefore, developing novel highly active and stable bifunctional catalysts is currently indispensable for the STD conversion.

3.2. Supported Bifunctional Catalyst for the STD Process. *3.2.1. Conventional Supported Catalyst.* In addition to the hybrid catalyst, the supported one, comprising Cu/ZnO as supported metals and a solid-acid as support, is also commonly employed in the STD reactions. Thus, the tandem process from syngas to DME is achieved in one bifunctional catalyst by a combination of two different active sites on the surface of one particle of the catalyst. Unlike the hybrid one, supported zeolite-based catalysts generally exhibit excellent physical properties and heat stability due to the high surface area and developed porosity of support, such as zeolite.

A conventional supported catalyst for the STD reaction can be prepared by the coprecipitation,[69,70] impregnation,[71] sol–gel,[72] coprecipitating sedimentation,[73] and other wet-chemical methods.[74−76] The features and activity of a STD catalyst strongly depend on the preparation method. In their latest work, Arnold et al. compared various catalyst preparation methods for the STD reactions, including coprecipitation-impregnation, impregnation, coprecipitation sedimentation, and oxalate coprecipitation.[75] The result clearly showed that catalysts prepared via the coprecipitation sedimentation and oxalate coprecipitation methods exhibited a better performance than those prepared by the coprecipitation impregnation and impregnation, as demonstrated in Figure 7a–b. The reason lies in several crucial

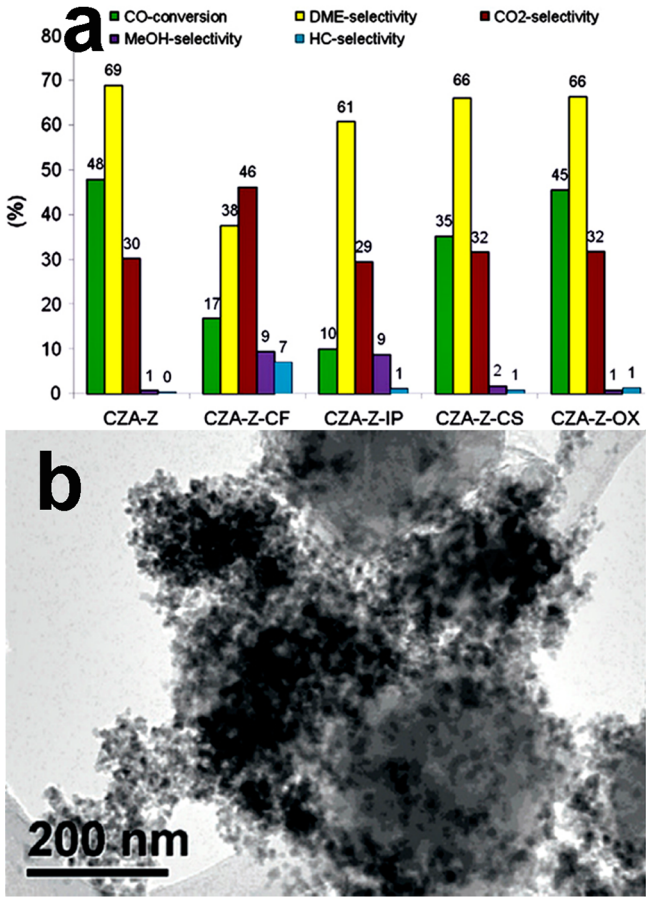

Figure 7. Catalysts for the STD reaction prepared by different methods. a) CO conversion and product selectivity for the various catalysts after 14 h on stream in STD reactions. (CZA-Z: admixed catalyst; CZA-Z-CF: coprecipitation impregnation; CZA-Z-IP: impregnation; CZA-Z-CS: coprecipitation sedimentation; CZA-Z-OX: oxalate coprecipitation); b) TEM images of the catalyst prepared by oxalate coprecipitation. Figures reproduced with permission from ref 75. Copyright 2014 Elsevier.

characteristics, such as higher Cu surface area and smaller Cu particle sizes as well as a higher number of moderate acidic sites, mentioned by many other relevant works as well.[71,77] Also, Moradi et al. found a most efficient preparation route for the $CuO/ZnO/Al_2O_3$ catalyst, namely the "sol-gel impregnation" method, by comparing several common preparation methods.[72] The advantage of this catalyst is attributed to the higher dispersion of metallic Cu (more specific surface area of Cu),

dx.doi.org/10.1021/cs500967j | ACS Catal. 2014, 4, 3346−3356

showing the best STD performance among various prepared catalysts.

In detail, the various precursors for Cu-based coprecipitated catalysts, such as copper nitrate, acetate, and chloride, can produce a significant effect on the bifunctional catalysis, as referred to by Lee and Bae et al.[70] In comparison with the bifunctional catalysts prepared from copper nitrate and copper chloride as starting resources, more acidic sites and a suitable surface area of metallic copper on the bifunctional Cu-based catalysts obtained from the copper acetate precursor is beneficial to achieve a better DME selectivity and catalytic activity, owing to the higher reaction rate of methanol dehydration to DME. In detail, the reaction rate and the DME yield showed an excellent relationship with the copper surface area multiplied with the amount of acidic sites, as illustrated in Figure 8.

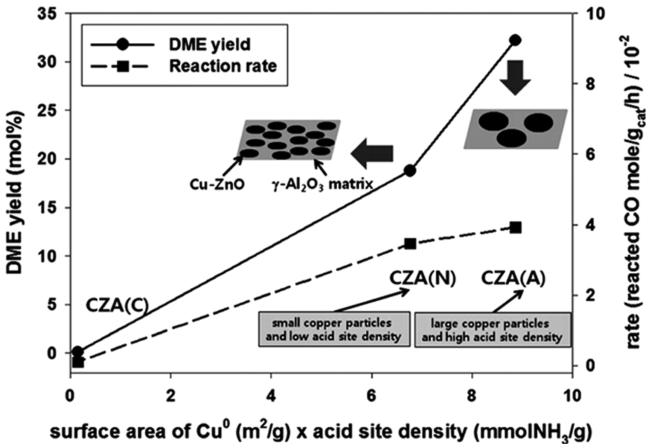

Figure 8. Correlation on the reaction rate and the DME yield to the copper surface area multiplied with the amount of acidic sites. Reproduced with permission from ref 70. Copyright 2011 American Chemical Society.

Apart from the role of acidic catalysis, zeolite also played an important role as the support of active Cu/ZnO components. A large BET surface area and pore volume of the dehydration catalyst are kinetically favorable to complete a high catalytic performance in DME synthesis. It is reported that employing H-MFI zeolite is more active and selective in the STD process than employing H-MOR, resulting from the higher pore volume and structure.[78] The pore volume of H-MFI 90 exceeds that of H-MOR 90 by a factor of 1.6. The former exhibits a three-dimensional pore structure, which is supposed to facilitate transport processes. Furthermore, coverage by more micropores on the H-MOR 90 surface can aggravate the accessibility of reactant molecules. The support effect on the STD catalytic performance is extremely complex and not completely clear, owing to the involvement of multiple factors (like porosity, interaction with the active metal, distribution location of metal particles), which determine the degree of metal reduction, the metal particle size, and its morphology.[79,80] It is worth being further identified in the aspect of the relationship between the multifunctional support and STD performance in the near future.

3.2.2. Bimetallic Physical Sputtering Catalyst. In several recent years, quite some emerging bifunctional catalysts of novel structure have been proposed and well developed, among which the physical sputtering catalyst is one of the most representative cases.[71,81−86] Traditionally, most of the wet-chemical preparation of STD catalysts consists of complicated steps, such as precipitation, filtration, washing, drying, and calcination at high temperature. Accordingly, supported active sites on a solid-acid support are nonuniform, distributed randomly on the support, even aggregated, and sintered after high-temperature calcination.[81,82] It is widely accepted that it is accessible to reactant molecules and available for catalysis, if a catalyst possesses smaller metal particles and larger exposed fraction of the metal atoms.[87] Beyond that, the active metals usually interact strongly with the acidic support, thus severely hindering the reduction of metal oxides or resulting in partial deactivation of catalysts.[86,88−90]

In light of the above, a series of highly dispersed metal/zeolite bifunctional catalysts were prepared through the self-made polygonal barrel sputtering route by our group, successfully applied in many typical tandem reactions of C1 chemistry, for instance, syngas to isoparaffins (based on Fischer−Tropsch synthesis)[81,86] and syngas to DME.[71,82]

As indicated in Figure 9a, the excited Ar plasma stream ceaselessly attacked the Cu−Zn bimetallic target, and the

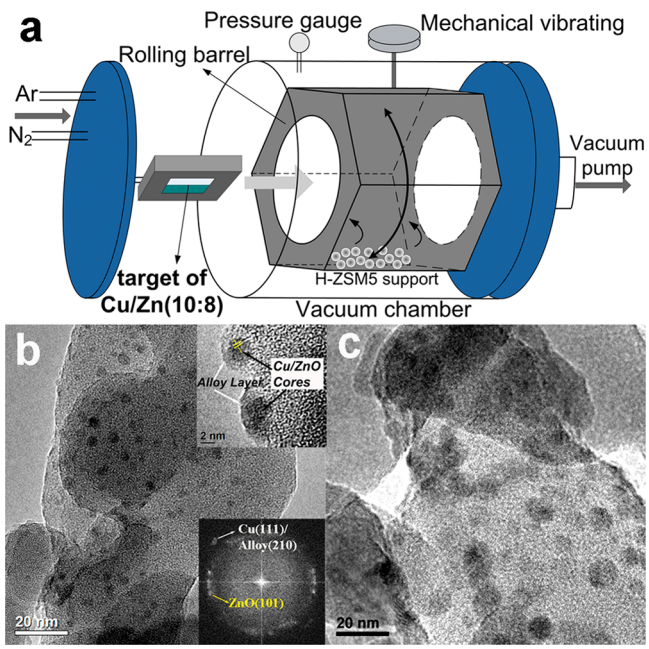

Figure 9. Schematic of the Cu−Zn sputtering apparatus (a), high-resolution TEM images of the sputtered catalyst (b) and impregnated catalyst (c). Figures reproduced with permission from ref 82. Copyright 2014 Royal Society of Chemistry.

obtained Cu and Zn atoms were deposited onto zeolite support. The hexagonal rotation and mechanical vibration during the physical sputtering accelerated the formation of highly dispersed and centered nanoparticles on zeolite support. By means of the continuous barrel rotation and mechanical vibration, each part of the rolling zeolite powders in barrel was provided enough chance to receive active Cu/Zn atoms, realizing homogeneous metal distribution.[82] Therefore, the spatial arrangement of the Cu/ZnO sites and acidic sites on zeolite could be optimized on the physically sputtered catalyst. The sputtered bifunctional catalyst was composed of well-dispersed Cu/ZnO nanoparticles of about 5 nm, which were physically anchored on the acidic zeolite support. More Cu surface areas are exposed on the sputtered catalyst than the impregnated one. A catalyst with a large Cu surface area can provide more effective active sites of methanol synthesis, accelerating CO conversion of the STD reaction. The

dx.doi.org/10.1021/cs500967j | ACS Catal. 2014, 4, 3346−3356

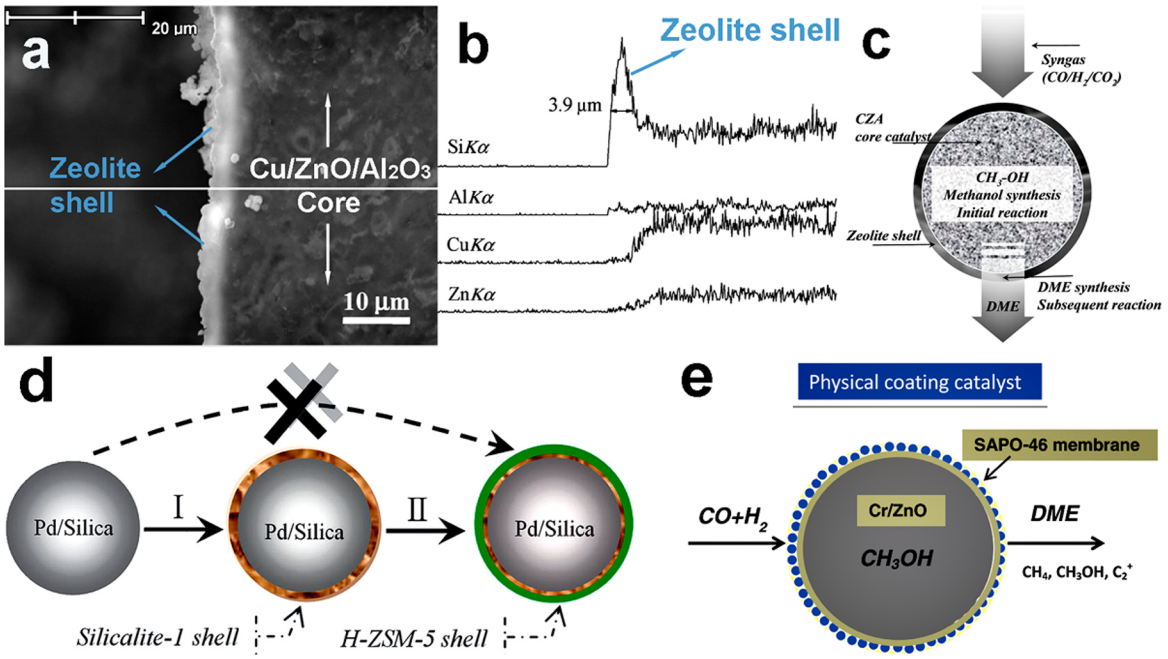

Figure 10. Capsule catalysts for DME synthesis. (a) Cross-section SEM image and (b) EDS line analysis of the zeolite capsule catalyst; (c) Reaction pathways and heat recycle on a single zeolite capsule catalyst; (d) Silica-based zeolite capsule via a dual-layer method; (e) A SAPO-46 encapsulated Cr/ZnO capsule catalyst by physically coating. Reprinted with permissions (a-c) from ref 67. Copyright 2010 American Chemical Society; (d) from ref 106. Copyright 2012 Royal Society of Chemistry; (e) from ref 107. Copyright 2013 Elsevier.

activity was found to increase with increasing the metallic Cu surface area to some extent, but it is not a simple linear relationship.[91] Furthermore, the weak interaction between physically anchored Cu/Zn nanoparticles and zeolite clearly decreased the reduction temperature by 50 °C.

In detail, after calcination and subsequent reduction, an active Cu_5Zn_8 nanoalloy layer was interestingly observed on Cu/ZnO nanoclusters, different from the impregnated one, as compared in Figures 9b and 9c. The surface alloying and well-dispersed Cu/ZnO nanoparticles played a cooperative catalytic role in improving STD performace, achieving a much higher DME selectivity and CO conversion than a conventional impregnated Cu-based catalyst. The "dry" sputtering route for catalyst preparation is a hopeful strategy to replace the conventional wet-chemical method, owing to its facile operation steps and being environmentally benign.

3.2.3. Zeolite Capsule Catalyst. For the conventional bifunctional STD catalysts, prepared by physical mixing, coprecipitation, or other wet-chemical methods, the different active sites distribute randomly in catalysts, as discussed in the previous part, providing an unrestricted and opened reaction environment.[92] Thus, the two coupled reactions are out of order and occurred independently, even though the distance between the two active sites is short.

Nowadays, the well-designed core−shell particles are driving interests in many promising applications, such as drug delivery,[93] fuel cells,[94] photonic devices,[95] photocatalysis,[96] and other revelant fields.[97−99] Inspired with the unique structure and properties, our group first developed a novel bifunctional catalyst with a unique core−shell structure, where the core and shell components independently catalyzed the different reactions and successfully applied in different heterogeneous catalysis.[67,100−104] Specifically for the STD reaction, the novel catalyst is composed of millimeter-sized alumina pellets supported Cu/ZnO/Al_2O_3 components as a core and a micron-sized HZSM-5 layer *in situ* grown on the surface of the core, called a "capsule catalyst". An aluminum-free route is presented to prepare the zeolite shell by employing an aluminum-containing core catalyst as the substrate for *in situ* acidic HZSM-5 zeolite shell growth, resulting in the defect-free covering and tightly enwrapping of the zeolite shell on the surface of the core catalyst.

Distinguishing from the hybrid and conventional supported catalysts, zeolite capsule catalysts exhibited a special core−shell structure, in which the acidic zeolite shell enwrapped the Cu/ZnO/Al_2O_3 core catalyst perfectly (Figure 10a−c). For the formed methanol from the internal Cu/ZnO/Al_2O_3 core, it is an unavoidable pathway to pass through the acidic zeolite shell owing to the spatial confinement effect.[92,105] Methanol is given enough opportunities to contact the active sites of the H-type zeolite shell and is converted into the expected DME product. Furthermore, the preliminary methanol synthesis reaction on the core catalyst and the following DME formation from methanol inside the zeolite shell cooperated concertedly and promoted mutually. The zeolite capsule catalyst with a synergetic confinement core−shell structure can be used to efficiently realize a tandem reaction with more synergistic effects.[67] In STD reactions, the zeolite capsule catalysts exhibited a striking promotion on DME selectivity as compared to the conventional mixture catalysts, suppressing the further dehydration of DME to form hydrocarbon byproducts, by the tailor-made acidic sites spatial arrangement.

Up to now, evolution of the capsule catalyst for the DME direct catalytic synthesis from syngas is still in progress, for instance, the silica-based zeolite capsule via a dual-layer method (Figure 10d),[106] silicoaluminophosphate (SAPO-46) encapsulated Cr/ZnO capsule catalyst by physically coating (Figure 10e),[107,108] etc. In summary, the concept of zeolite capsule catalyst demonstrated the unique effects of equilibrium shift, shape selectivity, and synergetic confinement in STD reactions. The DME selectivity of a capsule catalyst is comparable to other

dx.doi.org/10.1021/cs500967j | ACS Catal. 2014, 4, 3346−3356

Table 1. Comparison of Catalyst Performance Prepared by Different Methods

catalyst	preparation method	conversion %	DME sel.%	temp/°C	pressure/MPa	H_2/CO ratio	ref
CuZnAl+H-MFI400	physical mixture	48	69	250	5.1	1	75
CuZnAl+γ-Al_2O_3	physical mixture	61	67	250	5.1	2	78
CuFeZr+HZSM-5	physical mixture	28	65	260	3.0	5(H_2/CO_2)	55
CuZnAl/H-MFI400	coprecipitation impregnation	17	38	250	5.1	1	75
CuZnAl/H-MFI400	impregnation	10	61	250	5.1	1	75
CuZnAl/H-MFI400	oxalate coprecipitation	45	66	250	5.1	1	75
CuZnAl/γ-Al_2O_3	coprecipitation	66	49	250	5.0	2	70
CuZn/HZSM-5	sputtering	14	92	250	5.0	2	82
CuZnAl@HZSM-5	capsule	30	79	250	5.0	2	67
Pd-SiO_2@HZSM-5	capsule	9	69	250	5.0	2	106

new catalyst and conventional ones, as shown in Table 1. Consequently, it is promising to be widely extended for many other multiple-step consecutive reactions.

3.3. Evolution of Reaction Route of the STD Process. Fruitful efforts have been made in the improvement of catalyst construction for the STD process in the recent decade, as indicated in the previous parts. However, some crucial issues, for instance, the possible sintering and deactivation of catalysts from overheating in the highly exothermic STD reaction and further enhancement of CO/CO_2 one-pass conversion in STD, are not substantially solved as expected. Very few works have addressed so far the possible strategies to design new reaction routes for this issue.

Catalyst deactivation can be effectively avoided, and higher theoretic maximum CO/CO_2 conversion can be obtained by operating at low temperatures for STD reaction, in parallel with a long catalyst lifetime, less hydrocarbon byproducts, and lower energy consumption;[109] but methanol is industrially produced from syngas ($H_2/CO/CO_2$) under high temperatures and elevated pressures (250−300 °C, 5−10 MPa), with a typical Cu/ZnO-based catalyst.[63] To reduce the reaction temperature, changing the reaction route is effective by adding alcohol as a catalytic solvent, also a catalyst, which has been invented by our group.[9,63,110] The proposed new route is called "low-temperature methanol synthesis" (LTMS), depicted as below: $CO + H_2O \rightarrow CO_2 + H_2$; $CO_2 + H_2 + ROH \rightarrow HCOOR + H_2O$; $HCOOR + 2H_2 \rightarrow CH_3OH + ROH$. Coexisting alcohol (ROH) with reactants and catalysts in a slurry-bed reactor remarkably alters the reaction route from the conventional ICI process[8] to the proposed new route (Figure 11),[63] realizing the new low-temperature path (as low as 150 °C).

Based upon the LTMS route above, a novel low-temperature STD process with alcohol as the catalytic solvent and catalytic intermediate to change the reaction pathway is recently proposed by our group.[109] Methanol is selected as the solvent, catalyst, and also a product or an intermediate in this reaction, namely "self-catalysis". Based on a hybrid Cu/ZnO-based zeolite catalyst with assisted methanol, a CO conversion of 29% and 43% with a high DME selectivity of 69% and 68% was achieved at 170 or 180 °C, respectively. Most importantly, no other byproducts including methanol and hydrocarbons were observed. Of course, an appropriate amount of methanol was simultaneously required to accomplish the best STD catalytic stability, owing to its significant effect on the stability of STD reactions.

The novel low-temperature STD process combining the LTMS route provides a great potential for the future sustainable and economically viable production of DME. In a future large-scale industrial system, a high purity of DME will be well

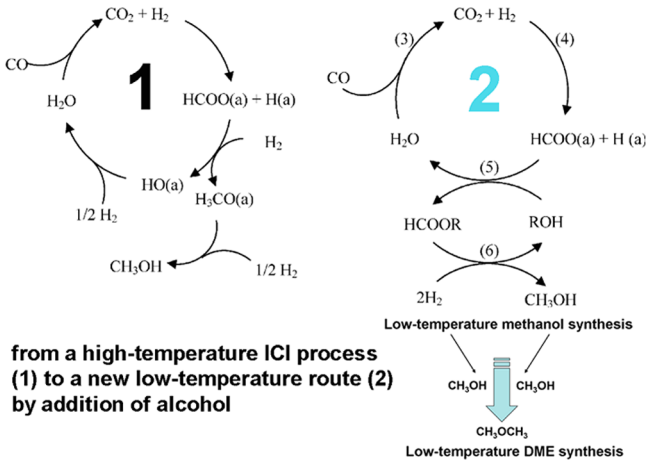

Figure 11. Low-temperature DME synthesis route based on the low-temperature methanol synthesis: changing the reaction course of methanol synthesis and DME synthesis from a high-temperature ICI process (1) to a new low-temperature route (2) by addition of alcohol.

predicted with less energy consumption, more stable reactions, and thus with both economic and environmental benefits.

3.4. Effect of Operating Conditions and Catalyst Deactivation. As a coupled tandem reaction, it is also necessary to investigate the effect of various reaction parameters such as temperature, pressure, H_2/CO ratio, and space velocity on CO conversion and DME selectivity. It is reported by Döring et al. that a temperature increase up to 280 °C, a higher H_2/CO in the synthesis gas, and a longer residence time will lead to a higher CO conversion.[78] DME selectivity is mainly dependent on the type of dehydration catalyst and can be influenced by temperature, residence time, and reaction pressure. The group of Ereña established kinetic models for the deactivation of the CuZnAl/γ-Al_2O_3 catalyst, allowing for calculating the effect of the operating conditions and the evolution of component concentration in the reaction medium with time on stream.[111,112] The deactivation kinetic model proposed is useful for future studies concerning the optimization of operating conditions, demonstrating that the STD reaction is very sensitive to these conditions. In detail, a significant increase in DME yield is available as the temperature is increased from 250 to 275 °C; the decrease in DME yield with time on stream occurs simultaneously to a clear increase in paraffin yield; the DME selectivity will reach maximum at the H_2/CO molar ratio of around 3/1; DME yield has a steady increase as pressure is increased, but deactivation is simultaneously faster due to the enhancement of coke condensation reactions.

dx.doi.org/10.1021/cs500967j | ACS Catal. 2014, 4, 3346−3356

Herein, the problem of reaction deactivation is unavoidable to most STD catalysts. The possible reasons for that are Cu sintering of Cu-based methanol synthesis catalyst and mainly coke deposition on the methanol dehydration catalyst.[113,114] This coke is presumably formed by degradation of methoxy ions (from DME or methanol et al.) generated from oxygenates in the reaction medium.[111,114] This hypothesis confirms that deactivation only has a direct effect on the methanol synthesis reaction and that deactivation kinetics is dependent on the concentration of oxygenates in the reaction medium.

The effect of water on the STD reaction has two opposite sides. First, it is considered that excessive water can decrease the methanol synthesis rate. Lee et al. reported that water influences both the methanol and the dehydration catalyst owing to the fact that adsorbed water blocks the active centers.[91] Han et al. also mentioned that water formed during the reaction deactivates the copper catalyst to a larger extent than the γ-Al_2O_3.[115] On the contrary, a suitable water amount will also hinder deactivation by coke deposition.[111] It is reported that in the case of moderate water addition (<10%), neither the CuZn-based catalyst nor solid acid catalyst exhibit rapid deactivation effects within several hours.[78] Therefore, it is important to control a suitable water amount for a more stable DME production in the future STD process.

In addition to water, incorporation of CO_2 in the CO-rich feed gas will influence the STD performance. In the presence of 8% CO_2 in syngas, approximately 10% lower CO conversion and about 5% lower DME selectivity are observed as compared to the reaction system without CO_2.[78] The addition of CO_2 can also considerably improve the long-term stability of the STD process,[116] but it is evident that the transformation of H_2 + CO_2 is significantly slower than that of H_2 + CO.[117]

4. INDUSTRIAL ADVANCES AND FUTURE PROSPECTS

Most of the above fundamental studies were performed on laboratory scale, whereas outstanding development for DME synthesis is also completed in industrial scale in recent years. Regarded as a clean fuel for the 21st century, DME has remarkable market and industrial potential, for electric power generation and for home energy source, such as heating and cooking, and is greatly cost-competitive with LPG and diesel fuel.

Plentiful DME production plants are developed worldwide, especially in the Asian area. The Haldor Topsoe, JFE Holdings, Air product & Chemical, and Korea Gas Corporation (KOGAS) have well representative plants in one-step conversion of syngas to DME. KOGAS employed an efficient one-step DME synthesis process from natural gas, consisting of CH_4 reformer section, CO_2 removal section, methanol regeneration section, DME reactor section, and DME purification section. The Toyo Engineering Co. developed a two-step technology for industrial DME production, comprising single train methanol synthesis and single train DME synthesis without an oxygen generator even in a large capacity DME plant of 3,500 tons per day.[12] It successfully builds several DME production plants, for instance, the plant of Sichuan Province and Shanxi Province in China. Figure 12a shows Japan's first DME production plant, which is located in Mitsubishi Gas Chemical's industrial facility in Niigata. The Fuel DME Production Company plant is a joint venture of a number of Japanese companies, including Mitsubishi Gas Chemical, Mitsubishi Heavy Industries, and Mitsubishi Chemical Company, and has a DME production capacity of 80,000 Ton per year.

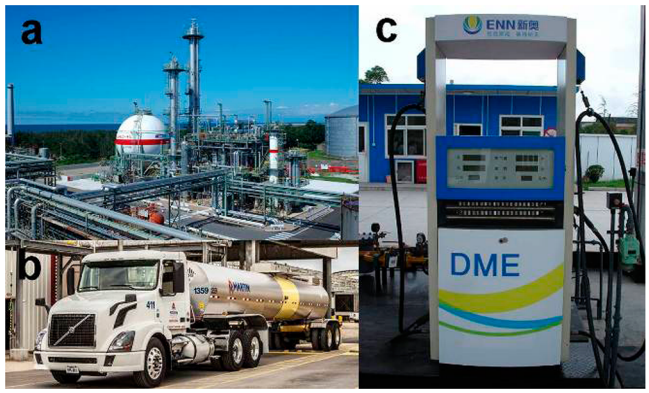

Figure 12. Representative DME production and applications worldwide. a) Japan's first DME production plant; b) Volvo production of DME heavy-duty trucks; c) a DME station in Shanghai, China.

The industrial DME application is also increasing based on the large-scale DME synthesis. In North America, Volvo starts production of DME heavy-duty trucks (Figure 12b). Following on the success of extensive DME fleet vehicle tests carried out in Europe, Volvo Trucks has become the first manufacturer to announce plans to commercialize DME-powered trucks in North America. In China, DME stations are tested by taxis in Minhang District of Shanghai City and a few local bus lines (Figure 12c),[118] as reported by the Shanghai Economic and Information Technology Commission.

Despite remarkable progress, some unsolved problems still remain in the MTD or STD reactions. For the case of MTD process, the acidity of alumina or zeolite is mainly modified with alkali metals, alkaline earth metals, transition metals, rare earth, and other composite oxides. Thus, enhancing the heat stability for a long time-on-stream in industrial production is worthy of consideration, in spite of the decrease of strong acid sites and byproduct after modification. Comparatively, the coupled one-step reaction from syngas to DME is a more promising strategy. However, further deep investigations are extremely necessary to optimize the ratio of two active catalyst components and identify the effect of interaction between Cu/ZnO-based sites and acidic sites. For the STD process, the hybrid catalyst is most developed and used currently. Recently, the bifunctional supported catalyst with better physical structure is emerging, showing a higher one-pass CO conversion and DME yield than conventional one. The precise design of catalyst construction is always crucial to the highly selective and active DME synthesis, regardless of the DME synthesis in lab-scale or industrial scale.

In addition, the profitability of DME production is heavily dependent on the raw material; therefore, in-depth studies of process technologies and economics with various feedstocks (e.g., natural gas, coal, biomass, or waste) are necessary. In other words, coupling with renewable sources for DME synthesis will be meaningful to the increasing energy and sustainable demands. We believe that after overcoming these problems in synthesis, growth in DME's use for domestic applications is expected to increase sharply, especially in developing countries where portable (bottled) fuel is providing a safer, cleaner, and more environmentally benign fuel for cooking and heating. Also, DME will become an efficient alternative of production of electric power for medium-sized power plants in the near future.

dx.doi.org/10.1021/cs500967j | ACS Catal. 2014, 4, 3346−3356

5. CONCLUSIONS

In light of the above, recent decades have witnessed the rapid development of DME catalytic synthesis. DME can be efficiently synthesized from methanol dehydration on a modified alumina or zeolite support. Modification with alkali metals, transition metals, rare earth, or other composite oxides is a excellent strategy to adjust acid strength and erase byproduct in MTD reactions. One-step conversion from syngas to DME is a booming area lately. Evolution of a catalyst structure for the STD process is obvious. Parallel with the conventional hybrid catalyst, a variety of unique bifunctional catalysts are developed, such as the $Cu/ZnO/Al_2O_3$@H-ZSM5 catalyst with a unique core−shell capsule structure and a bimetallic sputtered Cu/ZnO/H-ZSM5 one with a weak physical interaction between Cu/ZnO and zeolite. Optimizing catalyst structure, reaction conditions, and building kinetic models are necessary in the near future. Effect of catalyst properties, such as metal surface area, pore volume, and acidity, on kinetic behavior of DME synthesis is also important to be further investigated. To date, these important fundamental works are indispensible to the industrial application. With the increasing energy demands, it is believed that DME, a multiuse clean energy, will play more important roles in replacing LPG and diesel or serving for fuel cells.

AUTHOR INFORMATION

Corresponding Author

*Phone/Fax: +(81)-76-445-6846. E-mail: tsubaki@eng.u-toyama.ac.jp.

Notes

The authors declare no competing financial interest.

ACKNOWLEDGMENTS

The authors gratefully acknowledge financial support from the New Energy and Industrial Technology Development Organization (NEDO, Japan).

REFERENCES

(1) Olah, G. A.; Goeppert, A.; Prakash, G. K. S. *J. Org. Chem.* **2008**, *74*, 487−498.
(2) Song, W.; Marcus, D. M.; Fu, H.; Ehresmann, J. O.; Haw, J. F. *J. Am. Chem. Soc.* **2002**, *124*, 3844−3845.
(3) Liu, H.; Iglesia, E. *J. Phys. Chem. B* **2003**, *107*, 10840−10847.
(4) Cheung, P.; Bhan, A.; Sunley, G. J.; Iglesia, E. *Angew. Chem., Int. Ed.* **2006**, *45*, 1617−1620.
(5) Liu, H.; Cheung, P.; Iglesia, E. *J. Catal.* **2003**, *217*, 222−232.
(6) Li, X.; San, X.; Zhang, Y.; Ichii, T.; Meng, M.; Tan, Y.; Tsubaki, N. *ChemSusChem* **2010**, *3*, 1192−1199.
(7) Takeishi, K. *Biofuels* **2010**, *1*, 217−226.
(8) Behrens, M.; Studt, F.; Kasatkin, I.; Kuhl, S.; Havecker, M.; Abild-Pedersen, F.; Zander, S.; Girgsdies, F.; Kurr, P.; Kniep, B. L.; Tovar, M.; Fischer, R. W.; Norskov, J. K.; Schlogl, R. *Science* **2012**, *336*, 893−897.
(9) Shi, L.; Shen, W.; Yang, G.; Fan, X.; Jin, Y.; Zeng, C.; Matsuda, K.; Tsubaki, N. *J. Catal.* **2013**, *302*, 83−90.
(10) Arcoumanis, C.; Bae, C.; Crookes, R.; Kinoshita, E. *Fuel* **2008**, *87*, 1014−1030.
(11) Semelsberger, T. A.; Borup, R. L.; Greene, H. L. *J. Power Sources* **2006**, *156*, 497−511.
(12) Yoon, E. S.; Han, C. *Comput.-Aided Chem. Eng.* **2009**, *27*, 169−175.
(13) Liu, D.; Yao, C.; Zhang, J.; Fang, D.; Chen, D. *Fuel* **2011**, *90*, 1738−1742.
(14) Akarmazyan, S. S.; Panagiotopoulou, P.; Kambolis, A.; Papadopoulou, C.; Kondarides, D. I. *Appl. Catal., B* **2014**, *145*, 136−148.
(15) Yaripour, F.; Baghaei, F.; Schmidt, I.; Perregaard, J. *Catal. Commun.* **2005**, *6*, 147−152.
(16) Moses, P. G.; Nørskov, J. K. *ACS Catal.* **2013**, *3*, 735−745.
(17) Yang, Q.; Kong, M.; Fan, Z.; Meng, X.; Fei, J.; Xiao, F.-S. *Energy Fuels* **2012**, *26*, 4475−4480.
(18) Ladera, R. M.; Fierro, J. L. G.; Ojeda, M.; Rojas, S. *J. Catal.* **2014**, *312*, 195−203.
(19) Xu, M.; Lunsford, J. H.; Goodman, D. W.; Bhattacharyya, A. *Appl. Catal., A* **1997**, *149*, 289−301.
(20) Ladera, R.; Finocchio, E.; Rojas, S.; Busca, G.; Fierro, J.; Ojeda, M. *Fuel* **2013**, *113*, 1−9.
(21) DeWilde, J. F.; Chiang, H.; Hickman, D. A.; Ho, C. R.; Bhan, A. *ACS Catal.* **2013**, *3*, 798−807.
(22) Shi, B.; Davis, B. H. *J. Catal.* **1995**, *157*, 359−367.
(23) Roy, S.; Mpourmpakis, G.; Hong, D.-Y.; Vlachos, D. G.; Bhan, A.; Gorte, R. J. *ACS Catal.* **2012**, *2*, 1846−1853.
(24) Seo, C. W.; Jung, K. D.; Lee, K. Y.; Yoo, K. S. *Ind. Eng. Chem. Res.* **2008**, *47*, 6573−6578.
(25) Yaripour, F.; Baghaei, F.; Schmidt, I.; Perregaard, J. *Catal. Commun.* **2005**, *6*, 542−549.
(26) Yaripour, F.; Mollavali, M.; Jam, S. M.; Atashi, H. *Energy Fuels* **2009**, *23*, 1896−1900.
(27) Khom-in, J.; Praserthdam, P.; Panpranot, J.; Mekasuwandumrong, O. *Catal. Commun.* **2008**, *9*, 1955−1958.
(28) Laugel, G.; Nitsch, X.; Ocampo, F.; Louis, B. *Appl. Catal., A* **2011**, *402*, 139−145.
(29) Hassanpour, S.; Taghizadeh, M.; Yaripour, F. *Ind. Eng. Chem. Res.* **2010**, *49*, 4063−4069.
(30) Ramos, F.; Farias, A.; Borges, L. E. P.; Monteiro, J.; Fraga, M. A.; Sousa-Aguiar, E. F.; Appel, L. G. *Catal. Today* **2005**, *101*, 39−44.
(31) Vishwanathan, V.; Jun, K.-W.; Kim, J.-W.; Roh, H.-S. *Appl. Catal., A* **2004**, *276*, 251−255.
(32) Hassanpour, S.; Yaripour, F.; Taghizadeh, M. *Fuel Process. Technol.* **2010**, *91*, 1212−1221.
(33) Serrano, D. P.; Aguado, J.; Escola, J. M. *ACS Catal.* **2012**, *2*, 1924−1941.
(34) Yang, X.; Tiam, T. S.; Yu, X.; Demir, H. V.; Sun, X. W. *ACS Appl. Mater. Interfaces* **2011**, *3*, 4431−4436.
(35) Sun, H.-T.; Matsushita, Y.; Sakka, Y.; Shirahata, N.; Tanaka, M.; Katsuya, Y.; Gao, H.; Kobayashi, K. *J. Am. Chem. Soc.* **2012**, *134*, 2918−2921.
(36) Jin, D.; Zhu, B.; Hou, Z.; Fei, J.; Lou, H.; Zheng, X. *Fuel* **2007**, *86*, 2707−2713.
(37) Bezen, M. C. I.; Breitkopf, C.; Lercher, J. A. *ACS Catal.* **2011**, *1*, 1384−1393.
(38) Mao, R.; Le, T.; Fairbairn, M.; Muntasar, A.; Xiao, S.; Denes, G. *Appl. Catal., A* **1999**, *185*, 41−52.
(39) Han, S.; Shihabi, D. S.; Chang, C. D. *J. Catal.* **2000**, *196*, 375−378.
(40) Rownaghi, A. A.; Rezaei, F.; Stante, M.; Hedlund, J. *Appl. Catal., B* **2012**, *119*, 56−61.
(41) Ivanova, S.; Vanhaecke, E.; Louis, B.; Libs, S.; Ledoux, M.-J.; Rigolet, S.; Marichal, C.; Pham, C.; Luck, F.; Pham-Huu, C. *ChemSusChem* **2008**, *1*, 851−857.
(42) Li, C.; Xu, H.; Hou, S.; Sun, J.; Meng, F.; Ma, J.; Tsubaki, N. *Appl. Energy* **2013**, *107*, 297−303.
(43) Ha, K.-S.; Lee, Y.-J.; Bae, J. W.; Kim, Y. W.; Woo, M. H.; Kim, H.-S.; Park, M.-J.; Jun, K.-W. *Appl. Catal., A* **2011**, *395*, 95−106.
(44) Mollavali, M.; Yaripour, F.; Atashi, H.; Sahebdelfar, S. *Ind. Eng. Chem. Res.* **2008**, *47*, 3265−3273.
(45) Hytha, M.; Štich, I.; Gale, J. D.; Terakura, K.; Payne, M. C. *Chem.−Eur. J.* **2001**, *7*, 2521−2527.
(46) Carr, R. T.; Neurock, M.; Iglesia, E. *J. Catal.* **2011**, *278*, 78−93.
(47) Blaszkowski, S. R.; van Santen, R. A. *J. Phys. Chem. B* **1997**, *101*, 2292−2305.
(48) Lesthaeghe, D.; Van Speybroeck, V.; Marin, G. B.; Waroquier, M. *Angew. Chem., Int. Ed.* **2006**, *45*, 1714−1719.
(49) Mao, D.; Yang, W.; Xia, J.; Zhang, B.; Song, Q.; Chen, Q. *J. Catal.* **2005**, *230*, 140−149.

(50) Adachi, Y.; Komoto, M.; Watanabe, I.; Ohno, Y.; Fujimoto, K. *Fuel* **2000**, *79*, 229−234.
(51) Asadullah, M.; Ito, S.-i.; Kunimori, K.; Yamada, M.; Tomishige, K. *J. Catal.* **2002**, *208*, 255−259.
(52) Ashcroft, A.; Cheetham, A.; Green, M. *Nature* **1991**, *352*, 225−226.
(53) Minchener, A. J. *Fuel* **2005**, *84*, 2222−2235.
(54) Niu, M.; Huang, Y.; Jin, B.; Wang, X. *Ind. Eng. Chem. Res.* **2013**, *52*, 14768−14775.
(55) Liu, R.-w.; Qin, Z.-z.; Ji, H.-b.; Su, T.-m. *Ind. Eng. Chem. Res.* **2013**, *52*, 16648−16655.
(56) An, X.; Zuo, Y.-Z.; Zhang, Q.; Wang, D.-z.; Wang, J.-F. *Ind. Eng. Chem. Res.* **2008**, *47*, 6547−6554.
(57) García-Trenco, A.; Valencia, S.; Martínez, A. *Appl. Catal., A* **2013**, *468*, 102−111.
(58) Lu, W.-Z.; Teng, L.-H.; Xiao, W.-D. *Chem. Eng. Sci.* **2004**, *59*, 5455−5464.
(59) Clausen, L. R.; Elmegaard, B.; Ahrenfeldt, J.; Henriksen, U. *Energy* **2011**, *36*, 5805−5814.
(60) Takeguchi, T.; Yanagisawa, K.-i.; Inui, T.; Inoue, M. *Appl. Catal., A* **2000**, *192*, 201−209.
(61) Naik, S. P.; Du, H.; Wan, H.; Bui, V.; Miller, J. D.; Zmierczak, W. W. *Ind. Eng. Chem. Res.* **2008**, *47*, 9791−9794.
(62) Mao, D. S.; Yang, W. M.; Xia, J. C.; Zhang, B.; Lu, G. Z. *J. Mol. Catal. A: Chem.* **2006**, *250*, 138−144.
(63) Shi, L.; Yang, G.; Tao, K.; Yoneyama, Y.; Tan, Y.; Tsubaki, N. *Acc. Chem. Res.* **2013**, *46*, 1838−1847.
(64) Nakamura, J.; Choi, Y.; Fujitani, T. *Top. Catal.* **2003**, *22*, 277−285.
(65) Kasatkin, I.; Kurr, P.; Kniep, B.; Trunschke, A.; Schlögl, R. *Angew. Chem., Int. Ed.* **2007**, *46*, 7324−7327.
(66) Vidal, A. B.; Feria, L.; Evans, J.; Takahashi, Y.; Liu, P.; Nakamura, K.; Illas, F.; Rodriguez, J. A. *J. Phys. Chem. Lett.* **2012**, *3*, 2275−2280.
(67) Yang, G.; Tsubaki, N.; Shamoto, J.; Yoneyama, Y.; Zhang, Y. *J. Am. Chem. Soc.* **2010**, *132*, 8129−8136.
(68) Torres Galvis, H. M.; de Jong, K. P. *ACS Catal.* **2013**, *3*, 2130−2149.
(69) Tan, Y.; Xie, H.; Cui, H.; Han, Y.; Zhong, B. *Catal. Today* **2005**, *104*, 25−29.
(70) Baek, S.-C.; Kang, S.-H.; Bae, J. W.; Lee, Y.-J.; Lee, D.-H.; Lee, K.-Y. *Energy Fuels* **2011**, *25*, 2438−2443.
(71) Zeng, C.; Sun, J.; Yang, G.; Ooki, I.; Hayashi, K.; Yoneyama, Y.; Taguchi, A.; Abe, T.; Tsubaki, N. *Fuel* **2013**, *112*, 140−144.
(72) Moradi, G.; Nosrati, S.; Yaripor, F. *Catal. Commun.* **2007**, *8*, 598−606.
(73) Ge, Q.; Huang, Y.; Qiu, F.; Li, S. *Appl. Catal., A* **1998**, *167*, 23−30.
(74) Kang, S.-H.; Bae, J. W.; Kim, H.-S.; Dhar, G. M.; Jun, K.-W. *Energy Fuels* **2010**, *24*, 804−810.
(75) Ahmad, R.; Schrempp, D.; Behrens, S.; Sauer, J.; Döring, M.; Arnold, U. *Fuel Process. Technol.* **2014**, *121*, 38−46.
(76) Kang, S.-H.; Bae, J. W.; Jun, K.-W.; Potdar, H. *Catal. Commun.* **2008**, *9*, 2035−2039.
(77) Jung, J. W.; Lee, Y. J.; Um, S. H.; Yoo, P. J.; Lee, D. H.; Jun, K.-W.; Bae, J. W. *Appl. Catal., B* **2012**, *126*, 1−8.
(78) Stiefel, M.; Ahmad, R.; Arnold, U.; Döring, M. *Fuel Process. Technol.* **2011**, *92*, 1466−1474.
(79) Abelló, S.; Montané, D. *ChemSusChem* **2011**, *4*, 1538−1556.
(80) Cejka, J.; Corma, A.; Zones, S. *Zeolites and catalysis: synthesis, reactions and applications*; Wiley-VCH Verlag GmbH & Co. KGaA: Weinheim, Germany, 2010; 1056 pp.
(81) Sun, J.; Li, X.; Taguchi, A.; Abe, T.; Niu, W.; Lu, P.; Yoneyama, Y.; Tsubaki, N. *ACS Catal.* **2014**, *4*, 1−8.
(82) Sun, J.; Yang, G.; Ma, Q.; Ooki, I.; Taguchi, A.; Abe, T.; Xie, Q.; Yoneyama, Y.; Tsubaki, N. *J. Mater. Chem. A* **2014**, *2*, 8637−8643.
(83) Abe, T.; Tanizawa, M.; Watanabe, K.; Taguchi, A. *Energy Environ. Sci.* **2009**, *2*, 315−321.
(84) Sun, J.; Niu, W.; Taguchi, A.; Abe, T.; Yoneyama, Y.; Tsubaki, N. *Catal. Sci. Technol.* **2014**, *4*, 1260−1267.
(85) Jin, Y.; Yang, R.; Mori, Y.; Sun, J.; Taguchi, A.; Yoneyama, Y.; Abe, T.; Tsubaki, N. *Appl. Catal., A* **2013**, *456*, 75−81.
(86) Li, X.-G.; Liu, C.; Sun, J.; Xian, H.; Tan, Y.-S.; Jiang, Z.; Taguchi, A.; Inoue, M.; Yoneyama, Y.; Abe, T.; Tsubaki, N. *Sci. Rep.* **2013**, *3*, 2813.
(87) Gates, B. *Chem. Rev.* **1995**, *95*, 511−522.
(88) Farmer, J. A.; Campbell, C. T. *Science* **2010**, *329*, 933−936.
(89) de la Pena O'Shea, V. A.; Consuelo Alvarez Galvan, M.; Platero Prats, A. E.; Campos-Martin, J. M.; Fierro, J. L. G. *Chem. Commun.* **2011**, *47*, 7131−7133.
(90) Liu, X.; Liu, M.-H.; Luo, Y.-C.; Mou, C.-Y.; Lin, S. D.; Cheng, H.; Chen, J.-M.; Lee, J.-F.; Lin, T.-S. *J. Am. Chem. Soc.* **2012**, *134*, 10251−10258.
(91) Kim, H.-J.; Jung, H.; Lee, K.-Y. *Korean J. Chem. Eng.* **2001**, *18*, 838−841.
(92) Bao, J.; He, J.; Zhang, Y.; Yoneyama, Y.; Tsubaki, N. *Angew. Chem., Int. Ed.* **2008**, *47*, 353−356.
(93) Chen, L.; Li, L.; Zhang, L.; Xing, S.; Wang, T.; Wang, Y. A.; Wang, C.; Su, Z. *ACS Appl. Mater. Interfaces* **2013**, *5*, 7282−7290.
(94) Adijanto, L.; Sampath, A.; Yu, A. S.; Cargnello, M.; Fornasiero, P.; Gorte, R. J.; Vohs, J. M. *ACS Catal.* **2013**, *3*, 1801−1809.
(95) Mokkapati, S.; Saxena, D.; Jiang, N.; Parkinson, P.; Wong-Leung, J.; Gao, Q.; Tan, H. H.; Jagadish, C. *Nano Lett.* **2012**, *12*, 6428−6431.
(96) Li, J.; Cushing, S. K.; Bright, J.; Meng, F.; Senty, T. R.; Zheng, P.; Bristow, A. D.; Wu, N. *ACS Catal.* **2012**, *3*, 47−51.
(97) Ghosh Chaudhuri, R.; Paria, S. *Chem. Rev.* **2011**, *112*, 2373−2433.
(98) Li, G. L.; Mohwald, H.; Shchukin, D. G. *Chem. Soc. Rev.* **2013**, *42*, 3628−3646.
(99) Nie, R.; Lei, H.; Pan, S.; Wang, L.; Fei, J.; Hou, Z. *Fuel* **2012**, *96*, 419−425.
(100) Yang, G.; Kawata, H.; Lin, Q.; Wang, J.; Jin, Y.; Zeng, C.; Yoneyama, Y.; Tsubaki, N. *Chem. Sci.* **2013**, *4*, 3958−3964.
(101) He, J.; Liu, Z.; Yoneyama, Y.; Nishiyama, N.; Tsubaki, N. *Chem.−Eur. J.* **2006**, *12*, 8296−8304.
(102) Li, X.; Zhang, Y.; Meng, M.; Yang, G.; San, X.; Takahashi, M.; Tsubaki, N. *J. Membr. Sci.* **2010**, *347*, 220−227.
(103) He, J.; Yoneyama, Y.; Xu, B.; Nishiyama, N.; Tsubaki, N. *Langmuir* **2005**, *21*, 1699−1702.
(104) Li, X.; He, J.; Meng, M.; Yoneyama, Y.; Tsubaki, N. *J. Catal.* **2009**, *265*, 26−34.
(105) Sun, J.; Xing, C.; Xu, H.; Meng, F.; Yoneyama, Y.; Tsubaki, N. *J. Mater. Chem. A* **2013**, *1*, 5670−5678.
(106) Yang, G.; Wang, D.; Yoneyama, Y.; Tan, Y.; Tsubaki, N. *Chem. Commun.* **2012**, *48*, 1263−1265.
(107) Pinkaew, K.; Yang, G.; Vitidsant, T.; Jin, Y.; Zeng, C.; Yoneyama, Y.; Tsubaki, N. *Fuel* **2013**, *111*, 727−732.
(108) Yang, G.; Thongkam, M.; Vitidsant, T.; Yoneyama, Y.; Tan, Y.; Tsubaki, N. *Catal. Today* **2011**, *171*, 229−235.
(109) Reubroycharoen, P.; Teppood, S.; Vitidsant, T.; Chaiya, C.; Butnark, S.; Tsubaki, N. *Top. Catal.* **2009**, *52*, 1079−1084.
(110) Tsubaki, N.; Ito, M.; Fujimoto, K. *J. Catal.* **2001**, *197*, 224−227.
(111) Sierra, I.; Ereña, J.; Aguayo, A. s. T.; Olazar, M.; Bilbao, J. *Ind. Eng. Chem. Res.* **2010**, *49*, 481−489.
(112) Aguayo, A. T.; Ereña, J.; Mier, D.; Arandes, J. M.; Olazar, M.; Bilbao, J. *Ind. Eng. Chem. Res.* **2007**, *46*, 5522−5530.
(113) Sierra, I.; Ereña, J.; Aguayo, A. T.; Arandes, J. M.; Bilbao, J. *Appl. Catal., B* **2010**, *94*, 108−116.
(114) Sierra, I.; Olazar, M.; Gayubo, A. G.; Aguayo, A. T. *Ind. Eng. Chem. Res.* **2008**, *47*, 2238−2247.
(115) Wang, D.; Han, Y.; Tan, Y.; Tsubaki, N. *Fuel Process. Technol.* **2009**, *90*, 446−451.
(116) Sofianos, A. C.; Scurrell, M. S. *Ind. Eng. Chem. Res.* **1991**, *30*, 2372−2378.
(117) Ereña, J.; Garoña, R.; Arandes, J. M.; Aguayo, A. T.; Bilbao, J. *Catal. Today* **2005**, *107−108*, 467−473.
(118) Fleisch, T.; Basu, A.; Sills, R. *J. Nat. Gas Sci. Eng.* **2012**, *9*, 94−107.